Use of Technetium-99m-Liposomes in Tumor Imaging

Beth Goins, Robert Klipper, Alan S. Rudolph and William T. Phillips

Radiology Department, University of Texas Health Science Center at San Antonio, San Antonio, Texas and the Center for Biomolecular Science and Engineering, Naval Research Laboratory, Washington, D.C.

In this study, liposomes labeled with ^{99m}Tc have been evaluated as tumor imaging agents. **Methods:** Liposomes containing reduced glutathione and carrying either a negative surface charge or no surface charge were labeled with ^{99m}Tc using the lipophilic chelator, hexamethylpropyleneamine oxime (HMPAO). The ^{99m}Tc-liposomes were intravenously injected into the tail vein of nude mice which had been implanted intramuscularly in the thigh with nontransfected Chinese hamster ovary cells. Gamma camera images were acquired at 1, 4 and 22 hr and compared with tissue biodistribution studies at 24 hr postinjection. **Results:** Tumors could be distinguished from normal thigh muscle at 4 hr postinjection for both formulations. Tumor-to-muscle ratios were not significantly different for the two formulations due to the increased normal muscle activity at 24 hr for the neutral liposomes. Liver-to-tumor, liver-to-blood, spleen-to-tumor and spleen-to-blood ratios were significantly lower for the neutral ^{99m}Tc-liposomes than for the negative ^{99m}Tc-liposomes. Neutral ^{99m}Tc-liposomes were cleared slower by the reticuloendothelial system, and therefore remained in the circulation for a longer period of time. **Conclusion:** The results of this study indicate that both formulations could be used as tumor imaging agents, but that neutral ^{99m}Tc-liposomes would be more suitable as a drug delivery agent due to their increased total uptake by the tumor and decreased nonspecific uptake by the reticuloendothelial system.

Key Words: tumor imaging; technetium-99m; liposomes

J Nucl Med 1994; 35:1491–1498

The early and accurate detection of cancer is an important factor in the prognosis and treatment of the cancer patient (*1*). Noninvasive imaging can be used to stage cancer patients and allow for frequent and multiple imaging procedures over a broad time frame to assess the effectiveness of their treatment regimen. One research area has been in the use of liposomes containing radionuclides as tumor imaging agents (*2–4*). Liposomes are spherical lipid bilayers developed as drug delivery vehicles for chemotherapeutic drugs as well as radionuclides (*4*).

The trapping of radionuclides within the aqueous space of the liposome bilayer can occur by two mechanisms. First, liposomes containing radionuclides can be produced by adding the radionuclide during liposome formation. Second, radionuclide-containing liposomes can be produced by using a lipophilic chelator to carry the radionuclide across the lipid bilayer of preformed liposomes. Once across the membrane, the chelator can transfer the radionuclide to a second molecule previously encapsulated in the liposome. This second molecule has a greater affinity for the radionuclide than the chelator and acts to trap the radionuclide within the liposomal aqueous space. To date, the latter mechanism has been used by researchers to develop liposome radiopharmaceuticals containing ^{111}In, ^{67}Ga or ^{99m}Tc (*5–10*).

In this paper, we have used ^{99m}Tc-liposomes labeled with a newly developed method to evaluate the feasibility of using ^{99m}Tc-liposomes as a tumor imaging agent (*5*). This new procedure uses the lipophilic chelator, hexamethylpropyleneamine oxime (HMPAO) to carry ^{99m}Tc inside preformed liposomes containing reduced glutathione (GSH). The ^{99m}Tc-HMPAO molecule is thought to be chemically reduced in the presence of the GSH, becoming more hydrophilic and trapped within the liposome. This proposed liposome labeling mechanism may be similar to the mechanism of intracellular trapping of ^{99m}Tc-HMPAO by high concentrations of GSH in the brain (*11,12*).

The ^{99m}Tc-liposomes labeled using this method have been shown to be more stable in vivo than previously described ^{99m}Tc-liposomes used in clinical infection and cancer detection studies, which used surface labeling methods or encapsulated ^{99m}Tc chelated to diethylenetriamine pentaacetic acid (DTPA) (*13–20*). Another advantage of this ^{99m}Tc-liposome labeling technique appears to be that the ^{99m}Tc label is retained at the site of liposome deposition for prolonged periods without rapid metabolism. The prolonged retention results in improved image quality. Some of the advantages of using ^{99m}Tc over both ^{111}In and ^{67}Ga include availability, lower cost and better imaging characteristics (*19*). Also, the ^{111}In-liposome labeling procedure requires a high temperature incubation

Received Oct. 8, 1993; revision accepted Apr. 22, 1994.

For correspondence and reprints contact: William T. Phillips, MD, Radiology Dept., University of Texas Health Science Center at San Antonio, 7703 Floyd Curl Dr., San Antonio, TX 78284-7800.

which is not necessary for either the ^{99m}Tc-liposome or ^{67}Ga-liposome labeling procedure (*9*).

The influence of the radionuclide and chelator are not the only ingredients necessary for successful development of a useful liposomal-based tumor imaging agent (*21*). The physical characteristics of the liposome (lipid composition, surface charge and size) are all important components in the determination of the circulation properties following intravenous administration and must be taken into account when designing a tumor imaging agent (*22*). Each of these factors determines the extent of degradation of the liposomes by blood components such as serum and the removal of the liposomes by the reticuloendothelial system (RES) organs.

In the present study, a direct comparison of two ^{99m}Tc-liposome formulations for their ability to image tumors was carried out using a nude mouse tumor model. The neutral liposome formulation is the same as that found in one preparation of ^{111}In-liposomes approved as a tumor imaging agent (VesCan) (*9,10*). The other liposome formulation, which contains a negative surface charge, has been shown to localize at infection sites in rats (*23*). Our findings in this study indicate that both formulations are sufficient tumor imaging agents, but that the neutral liposome formulation had reduced uptake by the RES.

MATERIALS AND METHODS

Liposome Preparation

The liposomes were produced and characterized as outlined (*5*). The phospholipids, distearoyl phosphatidylcholine (DSPC) and dimyristoyl phosphatidylglycerol (DMPG), were purchased from Avanti Polar Lipids (Pelham, AL). Cholesterol was obtained from Calbiochem (La Jolla, CA) and alpha-tocopherol was purchased from Aldrich (Waukegan, IL). All liposomes used in this study were prepared by co-drying the lipids from chloroform prior to rehydration with 30 m*M* reduced glutathione (Sigma, St. Louis MO) in Dulbecco's phosphate-buffered saline (PBS), pH 7.4. The resultant multilamellar liposomes were passed through a microfluidizer (Microfluidics, Newton, MA) to form smaller and more unilamellar liposomes.

After processing, the liposomes were diluted with PBS, pH 7.4, and spun at 70,000 × g in a Beckman ultracentrifuge for 1 hr to remove any extravesicular GSH. Liposomes containing either a negative surface charge comprised of DSPC:cholesterol:DMPG:alpha:copherol (50:38:10:2 molar ratio) or no charge comprised of DSPC:cholesterol:alpha-tocopherol (66:32:2 molar ratio) were used in this study. Liposomal size was monitored using a Coulter N4-MD particle size analyzer (Hileah, FL). The average diameter for the neutral and negative liposomes was 155 ± 3 nm and 158 ± 2 nm, respectively. Phospholipid content of the liposomes was assayed using the method by Stewart (*24*). Liposomes were assayed for endotoxin and bacterial contamination on fluid thioglycollate media prior to labeling and injection. The intravesicular concentration of GSH has been estimated at 1.2 m*M* using [^{3}H] GSH (Du Pont New England Nuclear, Boston MA) (*5*).

Labeling Procedure

The ^{99m}Tc labeling procedure for preformed liposomes recently has been described (*5*). Briefly, approximately 10 ml of liposomes containing GSH were mixed with an HMPAO kit (Ceretec, Amersham, Arlington Heights, IL) preincubated with 10 mCi of sodium pertechnetate in 5 ml of 0.9% saline. The reconstituted kits were checked for contamination by free pertechnetate, reduced hydrolyzed ^{99m}Tc and hydrophilic ^{99m}Tc-HMPAO complex with the active lipophilic ^{99m}Tc-HMPAO complex using a three-step thin-layer chromatography system outlined in the HMPAO kit. In all cases, the kits used for the liposome labeling studies contained >80% lipophilic HMPAO as recommended for clinical brain studies. After a 30-min incubation, the liposomes were separated from any free ^{99m}Tc by passage over a Sephadex G-25 column.

Labeling efficiencies were checked by determining the activity before and after column separation of the ^{99m}Tc-liposomes using a dose calibrator (Radex Model Mark 5, Houston, TX). Also, chromatography on Schleicher and Schuell #589 chromatography paper developed in 0.9% saline was performed on pre- and postcolumn samples (*25*). With this technique, the liposomes remain at the origin while both free ^{99m}Tc and ^{99m}Tc-HMPAO move with the solvent front. The labeling efficiency of the postcolumn fractions of negative ^{99m}Tc-liposomes was 91%, while the efficiency was 72% for the neutral ^{99m}Tc-liposomes. The postcolumn preparations of ^{99m}Tc-liposomes were used immediately for injection.

Tumor Model

The animal experiments were performed under the National Institutes of Health Animal Use and Care guidelines and were approved by the University of Texas Health Science Center at San Antonio Institutional Animal Care Committee. Nontransfected Chinese hamster ovary cells were grown in Dulbecco's Modified Eagle media containing 10% heat-inactivated fetal calf serum. The cells were harvested with trypsin/EDTA, washed in saline and centrifuged at 500 × g. The number of cells was estimated by counting an aliquot of the diluted cell suspension in a hemocytometer. Female Balb c nu/nu nude mice (17–20 g) were injected intramuscularly in the thigh with 10^7 cells in 0.1 ml of saline. Mice were tested 10 days after tumor cell seeding. The average tumor weight at necropsy was 0.36 g. Tumor-bearing mice were anesthetized with Metofane (Pitman-Moore, Mundelein, IL) and injected intravenously in the tail vein with an average dose of either 50 μCi of negative ^{99m}Tc-liposomes or 37 μCi of neutral ^{99m}Tc-liposomes in a volume of 0.1 ml. The phospholipid dose was approximately 130 mg phospholipid/kg body weight.

Image Acquisition and Analysis

At 1, 4 and 22 hr, mice were anesthetized with Metofane and placed in the prone position for the imaging studies. Whole-body scintigrams were acquired using a Picker Model Dyna 4 gamma camera equipped with a high-resolution collimator (Picker International, Bedford, OH). The camera was interfaced to a Pinnacle computer (Medasys, Ann Arbor, MI) and 1-min static images were acquired using a 64 × 64 matrix and zoom of 3. Five-minute static images were acquired at 22 hr for mice injected with the ^{99m}Tc-liposomes. The animals were individually housed in metabolic cages immediately after receiving the ^{99m}Tc-liposomes and remained there until tissue biodistribution at 24 hr.

Regions of interest (ROIs) were drawn around the tumor in the thigh (tumor) and a comparable zone in the contralateral normal thigh (control) observed in the mouse images using the Pinnacle software. A box was drawn around the entire body to determine the total body counts. The target-to-background ratio was calculated using the following equation:

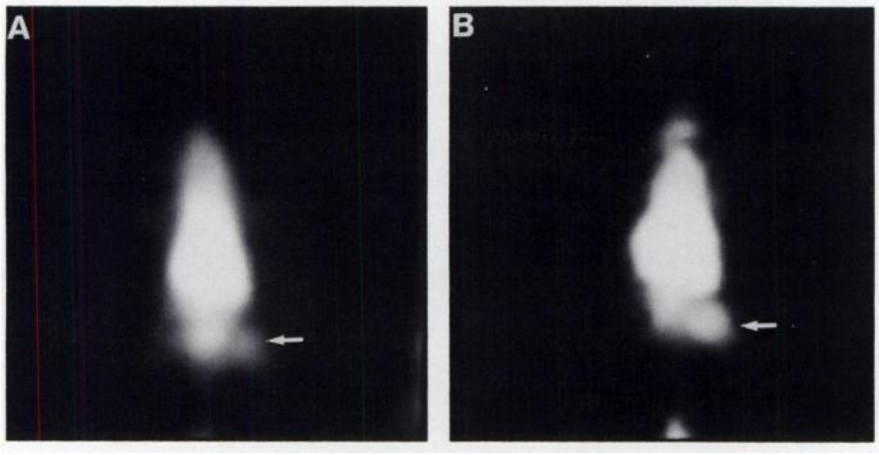

FIGURE 1. Serial whole-body gamma camera images of tumor-bearing nude mice injected with neutral ^{99m}Tc-liposomes and imaged at (A) 4 hr or (B) 22 hr postinjection.

$$\text{Target-to-Background Ratio} = \frac{\text{Counts (tumor)}}{\text{Counts (normal muscle)}}.$$

Also the activity at the tumor at various times was determined using the equation:

$$\%\ \text{activity in tumor} = \frac{\text{Counts (tumor)}}{\text{Counts (total body)}} \times 100.$$

Biodistribution Studies

After imaging, the animals were anesthetized with Metofane and a blood sample was obtained by cardiac puncture prior to death by cervical dislocation. Tissue samples were excised, thoroughly washed with saline and weighed. Samples of each organ were counted in a scintillation well counter (Canberra Multichannel Analyzer, Meridian, CT). A small sample of ^{99m}Tc-liposomes (0.1 ml) was placed in a plastic cuvette and used as a standard reference. Organ and fluid counts too high for detection at the time of death were stored until decay allowed for accurate determination. The bowel activity was determined by counting an aliquot of bowel digest after the total bowel plus contents were heated in the presence of saturated NaOH. Total blood volume, bone, muscle, brain and skin mass were estimated as 5.4%, 10%, 40%, 0.7% and 13% of total body weight, respectively (*26*).

Statistical Methods

Values are reported as mean ± standard error of the mean. Target-to-background ratios, % activity in the tumor and tumor-to-muscle ratios were compared for each liposomal formulation and at different time points using the Student's unpaired t-test. The acceptable probability for a significant difference between means was $p < 0.05$.

RESULTS

Nude mice bearing tumors in their left thigh were injected intravenously with ^{99m}Tc-liposomes containing no surface charge or a negative surface charge and imaged under a gamma camera to determine the extent of localization of the liposome formulations at the tumor site. Figure 1 shows representative gamma camera images of the tumor-bearing mice at 4 hr and 22 hr postinjection for the neutral ^{99m}Tc-liposome formulation. By 4 hr postinjection, the tumor can be delineated from the background muscle activity in the image and continued to improve by 22 hr postinjection. As shown in Figure 2, a similar delineation was seen in the 4-hr image of tumor-bearing mice receiving the negative ^{99m}Tc-liposomes which decreased somewhat by 22 hr postinjection.

The other major areas of accumulation of ^{99m}Tc-liposome activity were the RES organs of the liver and spleen, which are normal sites of clearance for liposomes (*22*). Also, the activity localized in the heart, which is representative of the cardiac blood pool, decreases by 22 hr in the

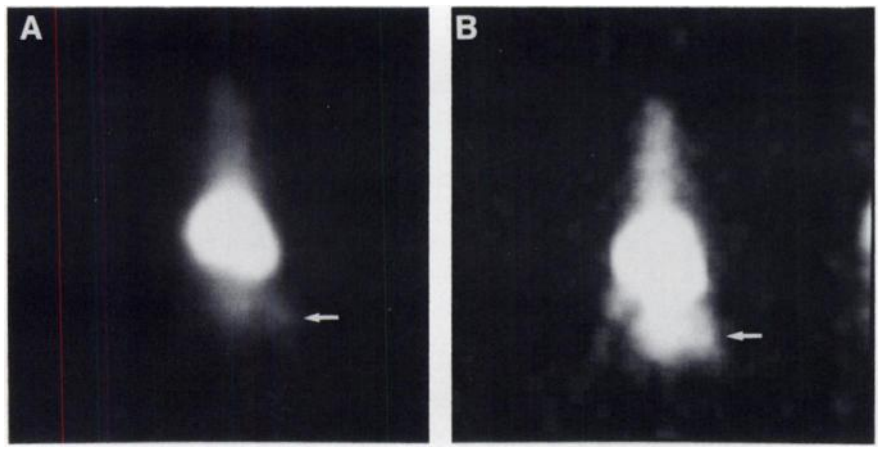

FIGURE 2. Serial whole-body gamma camera images of tumor-bearing nude mice injected with negative ^{99m}Tc-liposomes and imaged at (A) 4 hr or (B) 22 hr postinjection.

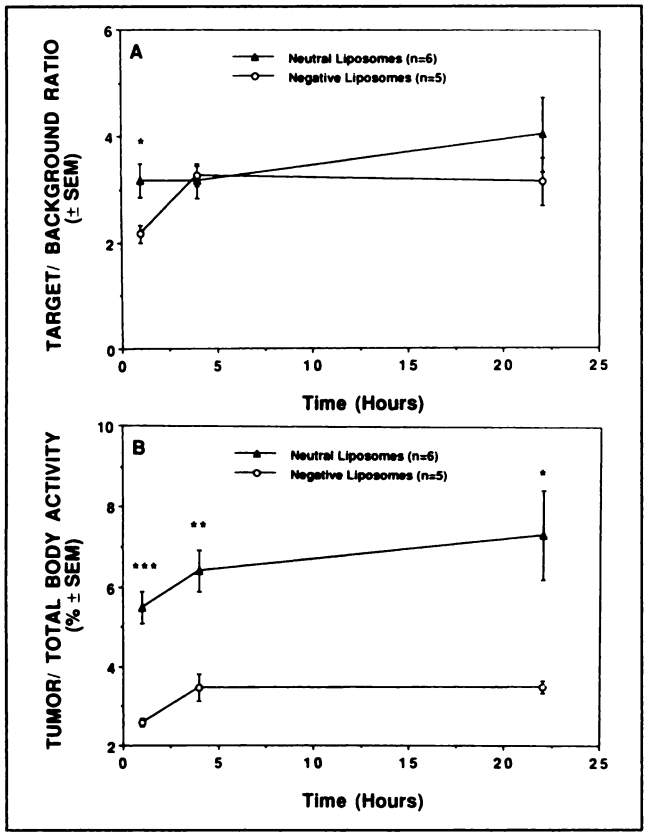

FIGURE 3. (A) Target-to-background ratios calculated from ROI image analysis of tumor-bearing mice injected with either neutral (n = 6) or negative (n = 5) ^{99m}Tc-liposomes and imaged over a 22-hr period. (B) Activity in the tumor of mice injected with either neutral (n = 6) or negative (n = 5) ^{99m}Tc-liposomes compared to total body activity over a 22-hr period. The activity was determined from ROI image analysis. The values represent the mean ± s.e.m. Differences considered to be statistically significant are indicated: * = $p < 0.05$; ** = $p < 0.01$; and *** = $p < 0.001$.

tumor-bearing mice receiving the negative ^{99m}Tc-liposomes, but remains constant for the neutral ^{99m}Tc-liposomes. This increased circulation persistence of the neutral ^{99m}Tc-liposomes may account for the increased accumulation of activity at the tumor site in the 22-hr image for the neutral ^{99m}Tc-liposomes. No significant activity was seen in the bladder, kidneys, thyroid or stomach for either ^{99m}Tc-liposome formulation, thus showing the excellent in vivo stability of ^{99m}Tc-liposomes using the labeling procedure outlined in this paper.

Target-to-background ratios were calculated from the images acquired over the 22-hr period for tumor-bearing mice receiving either the neutral or negative ^{99m}Tc-liposomes. As depicted in Figure 3A, the 1-hr target-to-background ratio of 3.2 ± 0.3 for the neutral ^{99m}Tc-liposomes was significantly greater than the target-to-background ratio of 2.2 ± 0.2 for the negative ^{99m}Tc-liposomes ($p < 0.05$). Similar target-to-background ratios of 3.2 ± 0.3 for the neutral ^{99m}Tc-liposomes and 3.3 ± 0.2 for the negative ^{99m}Tc-liposomes were determined at 4 hr. By 22 hr postinjection, the neutral ^{99m}Tc-liposomes continued to increase to a value of 4.0 ± 0.7, while the negative ^{99m}Tc-liposomes decreased to a value of 3.1 ± 0.5.

The activity at the tumor site was compared to the total body activity (Fig. 3B) for the two liposome formulations as a measure of tumor localization of the ^{99m}Tc-liposomes. As noted by other researchers (*27*), the percent activity localized at the tumor site for the neutral ^{99m}Tc-liposomes was significantly greater than for the negative ^{99m}Tc-liposomes at each time point (1 hr, $p < 0.001$; 4 hr, $p < 0.01$; and 22 hr, $p < 0.05$). For the neutral liposomes, there was no significant effect of time on the percent activity although the trend was increasing with values of 5.5% ± 0.4% at 1 hr, 6.4% ± 0.5% at 4 hr and 7.3% ± 1.1% at 22 hr. In contrast, there was a significant increase in the percent activity for the negative ^{99m}Tc-liposomes of 2.6% ± 0.1% at 1 hr to 3.5% ± 0.3% by 4 hr ($p < 0.05$) and remained at 3.5% ± 0.2% at 22 hr postinjection ($p < 0.001$).

Table 1 shows the tissue biodistribution data for ^{99m}Tc-liposomes injected in tumor-bearing mice sacrificed at 24 hr postinjection. The percent injected dose per organ determined from activity measurements of excised tissue confirm the image organ distribution patterns. There was a significantly greater percentage of the dose in the reticuloendothelial organs of the spleen ($p < 0.001$) and liver ($p < 0.001$) for the negative ^{99m}Tc-liposomes than for the neutral ^{99m}Tc-liposomes. On a per gram of tissue basis, there was 157% ± 11.5% of the activity in the spleen for the negative ^{99m}Tc-liposomes compared to 54.6% ± 5.2% in the spleen for the neutral ^{99m}Tc-liposomes. For the liver there was also a greater percentage of the activity on a per gram basis for the negative ^{99m}Tc-liposomes (25.1% ± 3.2%) than for the neutral ^{99m}Tc-liposomes (18.8% ± 0.9%). This result is consistent with other investigations showing neutral liposomes evading the RES better than liposomes containing a negative surface charge (*9,27*).

In contrast to the results for the liver and spleen, there was a greater percentage of the total activity remaining in the femur ($p < 0.05$) for the neutral ^{99m}Tc-liposomes (2.7% ± 0.2%) than for the negative ^{99m}Tc-liposomes (1.9% ± 0.3%). Our previous studies have shown that 90% of the activity in the femur is located in the marrow fraction, which is a secondary RES deposition site (*28*). There was also a significantly greater percentage of the dose remaining in the blood pool ($p < 0.001$) at 24 hr for the neutral ^{99m}Tc-liposomes (12.8% ± 1.9%) than for the negative ^{99m}Tc-liposomes (2.8% ± 0.5%). This result is in agreement with the image data at 22 hr (Figs. 1B and 2B) in which more activity is present in the heart region, which represents the circulating blood pool, for the neutral ^{99m}Tc-liposomes.

Tumor-bearing mice receiving neutral ^{99m}Tc-liposome also had significantly more activity than negative ^{99m}Tc-liposomes in the kidney ($p < 0.01$), lung ($p < 0.001$), heart ($p < 0.01$), brain ($p < 0.05$), skin ($p < 0.01$), ovary ($p < 0.01$) and bowel ($p < 0.001$). The increased activity in these organs is most likely due to the higher percentage of activity in the blood pool for the neutral ^{99m}Tc-liposomes, sug-

TABLE 1
Tissue Biodistribution of ^{99m}Tc-Liposomes at 24 Hours Postinjection

Organ	Neutral ^{99m}Tc-liposomes (n = 6)		Negative ^{99m}Tc-liposomes (n = 5)	
	%/organ	%/gram tissue	%/organ	%/gram tissue
Spleen	5.5 ± 0.4*	54.6 ± 5.2*	12.9 ± 0.8	157.1 ± 11.5
Lung	0.4 ± 0.04*	3.3 ± 0.4†	0.2 ± 0.01	1.1 ± 0.1
Liver	17.2 ± 0.9*	18.8 ± 0.9	22.6 ± 1.5	25.1 ± 3.2
Blood	12.8 ± 1.9†	12.2 ± 1.9†	2.8 ± 0.5	2.8 ± 0.4
Femur	2.7 ± 0.2‡	1.4 ± 0.1	1.9 ± 0.3	1.0 ± 0.1
Heart	0.3 ± 0.03†	2.7 ± 0.3†	0.1 ± 0.01	0.8 ± 0.1
Brain	0.1 ± 0.01‡	0.3 ± 0.1†	0.02 ± 0.004	0.1 ± 0.01
Skin	13.1 ± 2.0†	5.2 ± 0.9†	2.9 ± 0.4	1.2 ± 0.1
Kidney	1.9 ± 0.2†	7.7 ± 1.0‡	1.3 ± 0.2	4.6 ± 1.0
Urine	2.8 ± 0.4	0.3 ± 0.04	2.3 ± 0.4	0.2 ± 0.03
Bowel	5.9 ± 0.4*	2.2 ± 0.1†	2.9 ± 0.4	1.3 ± 0.1
Ovaries	0.07 ± 0.01†	2.2 ± 0.3‡	0.03 ± 0.01	1.0 ± 0.1
Feces	14.6 ± 1.3	11.6 ± 1.0	11.7 ± 1.5	13.1 ± 1.7
Muscle	4.8 ± 0.8†	0.6 ± 0.1†	1.4 ± 0.1	0.2 ± 0.01
Tumor	1.3 ± 0.3†	3.6 ± 0.3*	0.5 ± 0.2	1.0 ± 0.2
Tumor-to-muscle ratio	—	6.5 ± 0.8	—	5.2 ± 0.7

*$p < 0.001$ versus negative ^{99m}Tc-liposomes.
†$p < 0.01$.
‡$p < 0.05$.
Values represent the mean ± standard error.

gesting that the increased circulation allows more liposomes to eventually become deposited in these organs. In addition, the percent injected dose located in the muscle ($p < 0.01$) and tumor ($p < 0.01$) of tumor-bearing mice was significantly greater for the neutral ^{99m}Tc-liposomes than for the negative ^{99m}Tc-liposomes. There was no significant difference in the activity of urine ($p = 0.63$) or feces ($p = 0.17$) between the two liposome formulations.

The tumor-to-muscle and tumor-to-blood ratios at 24 hr calculated from the tissue biodistribution data for the ^{99m}Tc-liposome formulations are shown in Figure 4. The tumor-to-muscle ratio of 6.5 ± 0.8 for neutral ^{99m}Tc-liposomes was greater, but not significantly different from the ratio of 5.2 ± 0.7 for the negative ^{99m}Tc-liposomes. This result agrees with the target-to-background ratios calculated from the image data determined at 22 hr postinjection (Fig. 3A). Also the tumor-to-blood ratio for the neutral ^{99m}Tc-liposomes of 0.3 ± 0.04 was not statistically different from the ratio of 0.4 ± 0.1 for the negative ^{99m}Tc-liposomes.

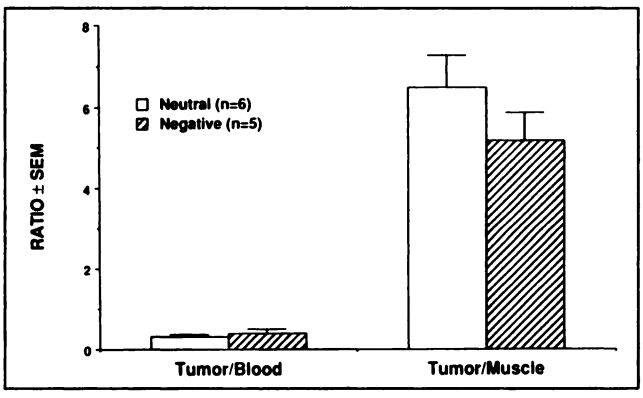

FIGURE 4. Tumor-to-muscle or tumor-to-blood ratios calculated from necropsy biodistribution data at 24 hr postinjection for tumor-bearing mice receiving either neutral (n = 6) or negative (n = 5) ^{99m}Tc-liposomes. The values represent the mean ± s.e.m.

Figure 5A depicts the liver-to-blood and liver-to-tumor ratios for both formulations at 24 hr postinjection. There was a significantly greater activity in the liver compared to the blood pool for the negative ^{99m}Tc-liposomes than for the neutral ^{99m}Tc-liposomes ($p < 0.001$). This result is in agreement with the organ distribution depicted in the gamma camera images (Figs. 1 and 2) showing more RES activity in the tumor-bearing mice receiving the negative ^{99m}Tc-liposomes. The liver-to-tumor ratio of 28.5 ± 3.7 for the negative ^{99m}Tc-liposomes was significantly greater than the ratio of 5.3 ± 0.4 for the neutral ^{99m}Tc-liposomes ($p < 0.001$). This ratio is approximately six times greater for the negative ^{99m}Tc-liposomes than for the neutral ^{99m}Tc-liposomes. This increase is due to less localization of the negative ^{99m}Tc-liposomes at the tumor, as well as a greater uptake of the negative ^{99m}Tc-liposomes in the liver.

In addition to the increased RES activity contributed by the liver for the negative ^{99m}Tc-liposomes, there was also a significant increase in spleen activity for the negative ^{99m}Tc-liposomes over the neutral ^{99m}Tc-liposomes. As shown in Figure 5B, both the spleen-to-blood and spleen-to-tumor ratios were significantly

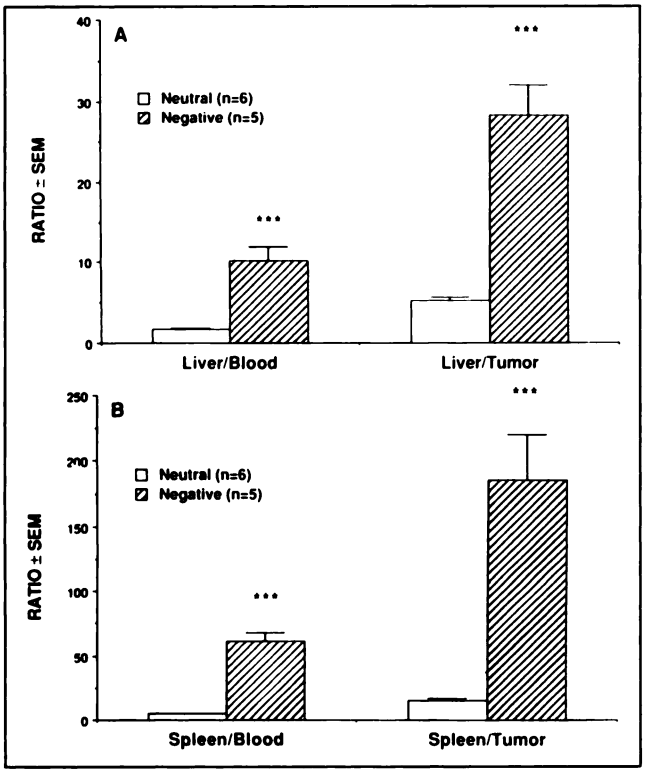

FIGURE 5. (A) Liver-to-blood and liver-to-tumor ratios calculated from necropsy biodistribution data at 24 hr postinjection for tumor-bearing mice receiving either neutral (n = 6) or negative (n = 5) ^{99m}Tc-liposomes. (B) Spleen-to-blood and spleen-to-tumor ratios calculated from necropsy biodistribution data at 24 hr postinjection for tumor-bearing mice receiving either neutral (n = 6) or negative (n = 5) ^{99m}Tc-liposomes. The values represent the mean ± s.e.m. Differences considered to be statistically significant are indicated: *** = $p < 0.001$.

greater ($p < 0.001$) for the negative ^{99m}Tc-liposomes than for the neutral ^{99m}Tc-liposomes. The spleen-to-blood ratio of 61.1 ± 6.5 for the negative ^{99m}Tc-liposomes was approximately 13 times greater than the ratio of 4.8 ± 0.5 for the neutral ^{99m}Tc-liposomes. The spleen-to-tumor ratio was 185.1 ± 35 and 15.3 ± 1.2 for the negative ^{99m}Tc-liposomes and neutral ^{99m}Tc-liposomes, respectively.

DISCUSSION

This study addresses the use of ^{99m}Tc-liposomes carrying either a negative or neutral surface charge as tumor imaging agents. The liposomes were labeled using a new ^{99m}Tc labeling method which provides for greater in vivo stability than previous ^{99m}Tc-liposome labeling techniques which either labeled the liposomal surface or encapsulated an unstable chelate (*13–20*). As a tumor imaging agent, in vivo stability is an important consideration because sufficient liposomes must remain in circulation for contact with the tumor. An early release of radionuclide with subsequent clearance through the bladder and bowels would result in a smaller percentage of activity available for targeting to the tumor site. By 24 hr only 2%–3% of the total activity is associated with the urine and 12%–15% with the feces.

The liposome labeling procedure used in this study employed ^{99m}Tc as the radionuclide rather than ^{67}Ga or ^{111}In. There are a number of advantages for using ^{99m}Tc over these other common radionuclides due to the inherent characteristics of each individual radionuclide. For example, the in vivo distribution of ^{99m}Tc is very different when it is associated with the liposome than when it is alone in circulation. When ^{99m}Tc-liposomes release the radionuclide, the ^{99m}Tc will be excreted in the bowel, bladder and thyroid. On the contrary, both ^{111}In and ^{67}Ga are attracted to metal chelates in the body and once released from the liposome become bound to these metal chelates, thus distributing in the same organs as the original labeled liposomes. In addition, ^{67}Ga has been shown to have a high affinity for tumors. In previous studies using ^{67}Ga-liposomes, the accumulation of ^{67}Ga at the tumor site was greater than the accumulation of the liposomes (*29*), indicating that the biodistribution determined was not the actual biodistribution of the ^{67}Ga-liposomes. Other advantages of using ^{99m}Tc to label liposomes over the radionuclides, ^{67}Ga and ^{111}In, include the fact that ^{99m}Tc is more readily available, costs less, has a 6-hr half-life for better dosimetric characteristics, and has a better energy for imaging studies (*19*). Moreover, the 6-hr half-life of ^{99m}Tc possibly would allow for higher imaging activities because the imaging is performed earlier.

Although both liposome formulations could be labeled using the ^{99m}Tc-liposome labeling protocol, there were differences in the rate of clearance of the liposome samples from the circulation. These findings agree with those of other researchers studying liposomes as drug delivery vehicles (*27*). Neutral liposomes were cleared slower by the RES and maintained in the bloodstream longer than the negative liposomes. The longer circulation times of the neutral ^{99m}Tc-liposomes are more than likely responsible for the increased activity at the tumor in mice receiving the neutral ^{99m}Tc-liposomes as seen in the images in Figure 1 and in the higher percent activity in the tumor seen in Figure 3B. However, the increased circulation also contributes to the greater muscle contribution by the neutral ^{99m}Tc-liposomes. Tumor-to-muscle ratios were not significantly different for the two formulations although the tumors were more evident in the mice receiving the neutral ^{99m}Tc-liposomes. These results are in contrast to previous infection imaging studies in rats injected with the same negative ^{99m}Tc-liposome formulation. The abscess-to-muscle ratio in rats was 35 at 24 hr postinjection, while the tumor-to-muscle ratio for this same liposome formulation was 5.2 in the present study. The most likely reason for the increased accumulation of the liposomes in the abscess over the tumor is their distinct pathology. In the abscess model, there could be greater extravasation of the liposomes than in the tumor model, as well as liposome migration with leukocyte infiltration (*30*). The increased circulation of the neutral ^{99m}Tc-liposomes also adds to the overall

time needed for the background activity to clear. One technology under development to provide for more rapid tumor imaging uses a biotin-containing liposome to target the tumor followed by a subsequent avidin injection to clear the bloodstream (*31*).

The liver-to-blood and liver-to-tumor ratios determined from the tissue biodistribution studies agree with the greater involvement of the RES in the clearance of the negative ^{99m}Tc-liposomes. In addition to the increased accumulation of activity in the liver for the negative liposome formulation, there was also a larger accumulation of activity in the other major RES organ, the spleen. This result can be seen in Table 1 where the percent activity per gram of spleen is three times greater for the negative ^{99m}Tc-liposomes than for the neutral ^{99m}Tc-liposomes. Also the spleen-to-blood and spleen-to-tumor ratios were significantly greater for the negative ^{99m}Tc-liposomes than for the neutral ^{99m}Tc-liposomes. The involvement of the RES has remained an issue in the application of liposomes as drug delivery agents and as radiotracers. One issue has been whether the accumulation of the liposomes in these organs at saturating levels will be toxic and interfere with their host defense duties which may already be compromised in the cancer patient. Recent human clinical trials of ^{111}In-liposomes as a tumor imaging agent have been carried out with few adverse side effects noted (*32*). Also at issue is whether the accumulation of activity in the RES organs will mask the ability to detect tumors localized in this region. Although the circulation properties and organ biodistribution of both liposome formulations used in this study have been well documented, they are first generation formulations. More sophisticated liposome formulations with liposome surfaces coated with polyethylene glycol or a sugar-containing lipid currently under investigation have been shown to have lower accumulation of activity in the RES organs and higher accumulation levels at the tumor site (*7,8,27,33–34*). Also, an antibody to a known tumor antigen could be covalently attached to the liposomal surface to add specificity to the labeled liposome and improve the targeting ability needed in diagnostic imaging (*35*).

CONCLUSION

The ^{99m}Tc-liposomes evaluated in this report could be used as tumor imaging agents. Of the two formulations tested in this paper, the neutral ^{99m}Tc-liposomes would be preferred clinically, because it not only could detect the tumor, but it has less activity in the RES. In addition to the application of this ^{99m}Tc-liposome labeling technique to radionuclide imaging, this labeling method could also be used to test new liposomal-based chemotherapeutic drugs. Further development of this new ^{99m}Tc-liposome labeling technique in the application of tumor imaging will focus on many of the issues discussed.

ACKNOWLEDGMENTS

The authors thank Rose Marie Bernal, Giuseppe Favarato Jr, Dr. Theresa Guise and Dr. Gregory Mundy in the Department of Medicine for their help with setting up the tumor model used in this study; Cono Farias for photographing the images for this paper; and Richard Cliff at the Naval Research Laboratory for determining the diameter of the liposomes. This project was funded through a grant from the Naval Medical Research and Development Command.

REFERENCES

1. Wagner HN, Conti PS. Advances in medical imaging for cancer diagnosis and treatment. *Cancer* 1991;67:1121–1128.
2. Seltzer SE. The role of liposomes in diagnostic imaging. *Radiology* 1989; 171:19–21.
3. Caride VJ. Technical and biological considerations on the use of radiolabeled liposomes for diagnostic imaging. *Nucl Med Biol* 1990;17:35–39.
4. Lasic D. Liposomes. *American Scientist* 1992;80:20–31.
5. Phillips WT, Rudolph AS, Goins B, Timmons JH, Klipper R, Blumhardt R. A simple method for producing a technetium-99m-labeled liposome which is stable in vivo. *Nucl Med Biol* 1992;19:539–547.
6. Gabizon A, Huberty J, Straubinger RM, Price DC, Papahadjopoulos D. An improved method for in vivo tracing and imaging of liposomes using a gallium-67-desferoxamine complex. *J Liposome Res* 1989;1:123–135.
7. Gabizon A, Price DC, Huberty J, Bresalier RS, Papahadjopoulos D. Effect of liposome composition and other factors on the targeting of liposomes to experimental tumors: biodistribution and imaging studies. *Cancer Res* 1990; 50:6371–6378.
8. Woodle MC. Gallium-67-labeled liposomes with prolonged circulation: preparation and potential as nuclear imaging agents. *Nucl Med Biol* 1993; 20:149–155.
9. Proffitt RT, Williams LE, Presant CA, et al. Tumor-imaging potential of liposomes loaded with ^{111}In-NTA: biodistribution in mice. *J Nucl Med* 1983;24:45–51.
10. Patel KR, Tin GW, Williams LE, Baldeschwieler JD. Biodistribution of phospholipid vesicles in mice bearing Lewis lung carcinoma and granuloma. *J Nucl Med* 1985;26:1048–1055.
11. Ballinger JR, Reid RH, Gulenchyn KY. Technetium-99m-HMPAO stereoisomers: differences in interaction with glutathione. *J Nucl Med* 1988;29: 1998–2000.
12. Neirinckx RD, Burke JF, Harrison RC, Forster AM, Andersen AR, Lassen NA. The retention mechanism of technetium-99m-HMPAO: intracellular reaction with glutathione. *J Cereb Blood Flow Metab* 1988;8:504–512.
13. Morgan JR, Williams KE, Davies RL, Leach K, Thomson M, Williams LAP. Localisation of experimental staphylcoccal abscesses by ^{99m}Tc-labelled liposomes. *J Med Microbiol* 1981;14:213–217.
14. Morgan JR, Williams LA, Howard CB. Technetium-labeled liposome imaging for deep-seated infection. *Br J Radiol* 1985;58:35–39.
15. Richardson VJ, Jeyasingh K, Jewkes RF, Ryman BE, Tattersall MHN. Properties of ^{99m}Tc-labeled liposomes in normal and tumor-bearing rats. *Biochem Soc Trans* 1977;5:290–291.
16. Deliconstantinos G, Ramantanis G, Todorou DK. Interaction of ^{99m}Tc-labeled liposomes with Walker tumour cells in vitro. Liposome-mediated introduction of thaliblastine into resistant Walker tumour cells. *Gen Pharmac* 1983;14:407–411.
17. Richardson VJ, Ryman BE, Jewkes RF, et al. Tissue distribution and tumour localization of ^{99m}Tc-labelled liposomes in cancer patients. *Br J Cancer* 1979;40:35–43.
18. Lopez-Berestein G, Kasi L, Rosenblum MG, et al. Clinical pharmacology of ^{99m}Tc-labeled liposomes in patients with cancer. *Cancer Res* 1984;44: 375–378.
19. Barratt GM, Tuzel NS, Ryman BE. The labeling of liposomal membranes with radioactive technetium. In: Gregoriadis G, ed. *Liposome technology*, volume 2. Boca Raton, FL: CRC Press; 1984:94–105.
20. Espinola LG, Beaucaire J, Gottschalk A, Caride VJ. Radiolabeled liposomes as metabolic and scanning tracers in mice. II. Indium-111-oxine compared with ^{99m}Tc-DTPA, entrapped in multilamellar lipid vesicles. *J Nucl Med* 1979;20:434–440.
21. Ogihara-Umeda I, Sasaki T, Nishigori H. Development of a liposome-encapsulated radionuclide with preferential tumor accumulation—choice of radionuclide and chelating ligand. *Nucl Med Biol* 1992;19:753–757.
22. Scherphof GL. In vivo behavior of liposomes: interactions with the mono-

nuclear phagocyte system and implications for drug targeting. In: Juliano RL, ed. *Targeted drug delivery*. New York: Springer-Verlag; 1991:285–327.
23. Goins B, Klipper R, Rudolph AS, Cliff RO, Blumhardt R, Phillips WT. Biodistribution and imaging studies of technetium-99m-labeled liposomes in rats with focal infection. *J Nucl Med* 1993;34:2160–2168.
24. Stewart JCM. Colorimetric determination of phospholipids with ammonium ferrothiocyanate. *Anal Biochem* 1980;104:10–14.
25. New RRC. Paper chromatography of labeled liposomes In: New RRC, ed. *Liposomes: a practical approach*. New York: IRL Press; 1990:265.
26. Crispens CG. *Handbook on the laboratory mouse*. Springfield, IL: Charles C. Thomas; 1975:82–90.
27. Allen TM, Hansen C, Rutledge J. Liposomes with prolonged circulation times: factors affecting uptake by the reticuloendothelial system. *Biochim Biophys Acta* 1989;981:27–35.
28. Rudolph AS, Cliff RO, Klipper R, Goins B, Phillips, WT. Circulation persistence and biodistribution of lyophilized liposome encapsulated hemoglobin: an oxygen carrying resuscitative fluid. *Crit Care Med* 1994: in press.
29. Ogihara-Umeda I, Kojima S. Increased delivery of gallium-67 to tumors using serum-stable liposomes. *J Nucl Med* 1988;29:516–523.
30. Papahadjopoulos D. Optimal liposomal drug action: from serendipity to targeting. In: Gregoriadis G, ed. *Liposome technology*, volume 3. Boca Raton, FL: CRC Press; 1993:1–14.
31. Ogihara-Umeda I, Sasaki T, Nishigori H. Active removal of radioactivity in the blood circulation using biotin-bearing liposomes and avidin for rapid tumour imaging. *Eur J Nucl Med* 1993;20:170–172.
32. Presant CA, Ksionski G, Crossley R. Indium-111-labeled liposomes for tumor imaging: clinical results of the international liposome imaging study. *J Liposome Res* 1990;1:431–436.
33. Oku N, Namba Y, Takeda A, Okada S. Tumor imaging with technetium-99m-DTPA encapsulated in RES-avoiding liposomes. *Nucl Med Biol* 1993; 20:407–412.
34. Senior J, Delgado C, Fisher D, Tilcock C, Gregoriadis G. Influence of surface hydrophilicity of liposomes on their interaction with plasma protein and clearance from circulation: studies with poly(ethylene glycol)-coated vesicles. *Biochim Biophys Acta* 1991;1062:77–82.
35. Poste G. Liposome targeting in vivo: problems and opportunities. *Biol Cell* 1983;47:19–38.